

Attitude Stabilization in Hover Flight of a Mini Tail-Sitter UAV with Variable Pitch Propeller

K.C. Wong, J.A. Guerrero, D. Lara and R. Lozano

Abstract—In this paper, the modeling and control design of a vertical flight attitude control for a mini tail-sitter with variable pitch propeller is discussed. Tail-sitters VTOL-UAVs have operational flexibility of typical helicopters while having the cruise performance of fixed wing airplanes. The configuration proposed in this work is highly unstable in its natural flight state in vertical mode. A dynamic model is developed and a linear control strategy has been developed to stabilize the platform. The results are supported by experimental tests.

I. INTRODUCTION

The study and development of Unmanned Aerial Vehicles (UAVs) has matured over recent years due to the fact that they can be used in a wide variety of applications, ranging from environmental monitoring in civil applications to surveillance and homeland security in military applications. Usually UAVs are categorized as fixed wing conventional or hovering rotary-wing aircraft systems. On the one hand, fixed wing conventional aircrafts have proven reliability, long flight time and cruise efficiency but they cannot hover or fly at low speeds. On the other hand, hovering platforms have the operational flexibility of being able to take-off vertically, hover and land vertically, but they usually have limitations in forward flight, such as low speed and poor endurance. A relatively unexplored configuration for UAVs is the tail-sitter vehicle. Tail-sitters have more operational flexibility than conventional UAVs because a vertical airframe attitude is adopted during take-off and landing, while maintaining a horizontal airframe attitude during cruise just like conventional airplanes. Tail-sitters have not been as widely adopted as an aircraft configuration due to complex flight dynamics in the hover mode, making them typically very difficult to control. The Convair XF-Y1 and Lockheed XF-V1 were examples of experimental Tail-sitters aircraft in the 1950s, but they were unsuccessful mostly due to the problem caused by the awkward position of pilot required during the vertical flight phases, which would not be relevant for UAVs. In the 1990s Boeing presented its tail-sitter Heliwing UAV with a flight controller using cyclic-pitch rotor control for its vertical flight phases [1], while more recently in [2], the University of Sydney's T-Wing UAV has an autopilot which uses control surfaces in the slipstream of fixed-pitch propellers for control in its vertical flight phases. Another interesting configuration

can be found in [3], where a small conventional airplane is presented with a hover capability using propeller slipstream over conventional control surfaces. This vehicle uses an inertial measurement unit and an onboard control system to stabilize the flight attitude. However this configuration presents problems related with the gyroscopic effect and the yaw control which is unsolved.

In recent years, interest in Vertical Take-Off and Landing (VTOL) mini Air vehicles (mAVs) have increased significantly due to a desire to operate UAVs in an urban environment. Many concepts have been proposed globally [4]. The Bidule mAV was developed at the University of Sydney to explore design issues related to small flight platforms [5]. The latest version, the Bidule CSyRex, is a joint project between the University of Sydney and the University of Technology of Compiègne to develop a VTOL variant of the Bidule. The vertical flight schematic of this VTOL vehicle is shown in Figure 1, which is basically a fixed wing tailless aircraft with two propellers. In hover the altitude is controlled with the collective thrust, this means, the lift force is generated increasing the speed of the propellers. The pitch attitude angular displacement is achieved by moving the elevons in the same direction. The vertical yaw-attitude angular displacement is achieved through moving the elevons in opposing direction. The vertical roll-attitude angular displacement is controlled by changing the pitch angle of the Variable Pitch Propeller (VPP).

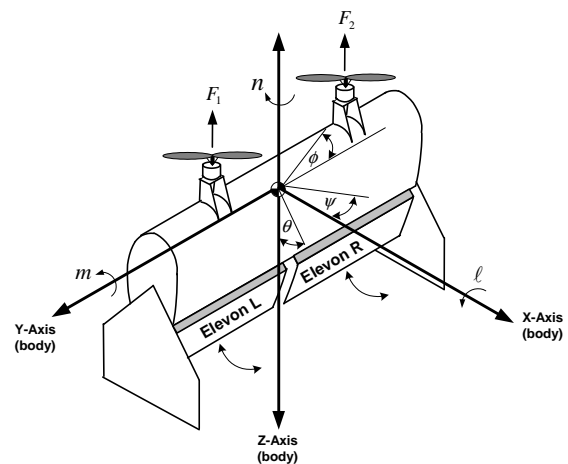


Fig. 1. Vehicle schematic for vertical flight mode of Bidule

Typically, mAVs, such as the Planar Vertical Takeoff and Landing (PVTOL) platforms [1] modify the speed of the DC electric motors to effect altitude and attitude control.

K.C. Wong is with School of Aerospace, Mechanical and Mechatronic Engineering, University of Sydney, Australia, kc@aeromech.usyd.edu.au; R. Lozano and J. A. Guerrero are with HEUDIASYC UMR 6599 CNRS-UTC, BP. 20529, CP. 60205 Compiègne, France. rlozano, jguerrero@hds.utc.fr; D. Lara is with Electronic Department at U.A.M.Reynosa-Rodhe, UAT, México dlara@uat.edu.mx

But when, brushless electric AC motors are used control responses have been too slow due to the time delay produced by the available speed controllers, leading to problems utilizing motor speed for roll control. VPP is thus being investigated as a potential solution, increasing the control response. This allows to implement a simple flight controller without considering the time-delay in actuators.

A main contribution of this work is to provide a simplified dynamic model of a VPP tail-sitter mAV using the Newton-Euler method while investigating the use of a linear controller to stabilize the attitude of the platform in vertical flight phases. This work is organized as follows: section II presents the general attitude dynamic model. In section III, three linear control systems are proposed. In section IV, the platform is described briefly. The experimental results are given in section V, and some simulation guidelines are described. Finally in section VI, the conclusions are presented.

II. VEHICLE ATTITUDE DYNAMIC MODEL

To obtain the vehicle attitude dynamical model, it will be assumed to be operated over a small local region on earth, justifying the utilization of the Flat-Earth model equations [6]. There are five equations representing the kinematics, the position, the forces and the moments, which are as follows.

$$C_{b/n} = fn(\Phi) \quad (1)$$

$${}^e \dot{\mathbf{p}}_{CM/T}^n = C_{n/b} \mathbf{v}_{CM/e}^b \quad (2)$$

$$\dot{\Phi} = H(\Phi) \omega_{b/e}^b \quad (3)$$

$${}^b \mathbf{v}_{CM/e}^b = \frac{\mathbf{F}_{A,T}^b}{m} + C_{b/n} \mathbf{g}^n - \Omega_{b/e}^b \mathbf{v}_{CM/e}^b \quad (4)$$

$${}^b \dot{\omega}_{b/e}^b = (J^b)^{-1} [\mathbf{M}_{A/T}^b - \Omega_{b/e}^b J^b \omega_{b/e}^b] \quad (5)$$

The vehicle center of mass, CM , is coincident with the body frame origin, F_b . The position of CM in the NED coordinate system with respect to the inertial frame origin, F_e , is given by $\mathbf{p}_{CM/T}^n = [p_N \ p_E \ p_D]^T$. The term $\mathbf{v}_{CM/e}^b = [U \ V \ W]^T$, represents the velocity in terms of the body components. The angular velocity in terms of the body system is given by $\omega_{b/e}^b = [P \ Q \ R]^T$ and its cross product matrix is denoted by $\Omega_{b/e}^b$. The angular velocity in the local inertial system has components $\dot{\Phi} = [\dot{\phi} \ \dot{\theta} \ \dot{\psi}]^T$. The aerodynamic and thrust force vector in the body system is represented by $\mathbf{F}_{A,T} = [X_{A,T} \ Y_{A,T} \ Z_{A,T}]^T$. The matrix of rotation (using the sequence z, y, x) from F_e to F_b is denoted by $C_{b/n}$.

The set of attitude equations can be obtained using the equations (3) and (5). The transformation of the components of the angular velocity generated by a sequence of Euler rotations from the body to the local reference system is written as follows:

$$H(\Phi) = \begin{bmatrix} 1 & t\theta s\phi & t\theta c\phi \\ 0 & c\phi & -s\phi \\ 0 & s\phi/c\theta & c\phi/c\theta \end{bmatrix} \quad (6)$$

where s and c are used to denote the sin and the cos respectively, then using (6), the *kinematic equations* (3) can

be rewritten as:

$$\dot{\phi} = P + \tan \theta (Q \sin \theta + R \cos \theta) \quad (7)$$

$$\dot{\theta} = Q \cos \phi - R \sin \phi \quad (8)$$

$$\dot{\psi} = (Q \sin \phi + R \cos \phi) / \cos \theta \quad (9)$$

The term J^b in (5) represents the inertia matrix, and is defined by

$$J^b = \begin{bmatrix} J_x & J_{xy} & J_{xz} \\ J_{yx} & J_y & J_{yz} \\ J_{zx} & J_{zy} & J_z \end{bmatrix}$$

If the Bidule CSyRex can be assumed to have the body axis xz -plane coincident with the plane of symmetry, then the products of inertia J_{xy} and J_{yz} vanishes. This tail-sitter configuration, also presents a plane of symmetry in the yz -plane, then the product of inertia $J_{xz} = 0$. Then J^b and its inverse can be written by

$$J^b = \begin{bmatrix} J_x & 0 & 0 \\ 0 & J_y & 0 \\ 0 & 0 & J_z \end{bmatrix} \text{ and } (J^b)^{-1} = \begin{bmatrix} \frac{1}{J_x} & 0 & 0 \\ 0 & \frac{1}{J_y} & 0 \\ 0 & 0 & \frac{1}{J_z} \end{bmatrix}$$

Note that the mass of the elevons is neglected. The aerodynamics and thrust moments can be denoted by $\mathbf{M}_{A,T}^b = [\ell \ m \ n]^T$, they are shown in the Figure 1, then using the matrix of inertia and the moment vector, the equation (5) yields:

$$\dot{P} = \frac{(J_y - J_z)QR}{J_x} + \frac{\ell}{J_x} \quad (10)$$

$$\dot{Q} = \frac{(J_z - J_x)RP}{J_y} + \frac{m}{J_y} \quad (11)$$

$$\dot{R} = \frac{(J_x - J_y)PQ}{J_z} + \frac{n}{J_z} \quad (12)$$

III. ATTITUDE CONTROL

This section presents three decoupled stability augmentation control systems for the roll, the pitch, and the yaw positions of the vehicle in hover flight. These subsystems will be obtained using only the kinematics and moment equations from the general model. Several aerodynamic factors will be taken into account to obtain the transfer function that represents the dynamic of each system.

A. Roll control

To obtain the roll control system, it is assumed that the pitch and yaw rates are zero. Then, the vehicle can be analyzed in a similar manner to a PVTOL flight platform, as in [1]. This configuration is shown in Figure 2. Therefore, using the equations (7) and (10), the rotational dynamics for the roll angle can be represented by:

$$\ddot{\phi} = \ell / J_x \quad (13)$$

where, the sum of moments ℓ can be calculated as follows:

$$\ell = F \cdot d - C_{\ell_\phi} \dot{\phi} \quad (14)$$

and $F = f_1 - f_2$ is the force difference between the right and left rotor and d is the distance from the center of mass to

each rotor. The second term in the right side of equation (14) represents an aerodynamic moment produced by the change of the roll rate, normally opposing to the roll moment, that is why, the derivative, $C_{l_{\dot{\phi}}} = 0.36$, is known as roll damping derivative. Then equation (13) can be rewritten as follows:

$$\ddot{\phi} = (F \cdot d - C_{l_{\dot{\phi}}} \dot{\phi}) / J_x \quad (15)$$

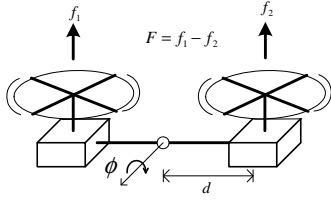


Fig. 2. Approach of PVTOL to control the roll position

The lift force in each rotor can be considered as the thrust and can be calculated by the following expression:

$$T = C_t \rho n^2 D^4 \quad (16)$$

where C_t is the thrust coefficient, ρ is the density of the air, n is the number of revolutions per second of the motor and D is the diameter of the propellers. The thrust coefficient is a function of the pitch angle propeller φ , which is shown in Figure 3. The thrust coefficient in a linear region can be calculated by:

$$C_t = C_{t_{\varphi}} \varphi \quad (17)$$

where $C_{t_{\varphi}}$ is a derivative which represents the thrust slope with respect to the VPP angle. This derivative has been estimated using a shareware program called JavaProp [7]. This program uses the number of blades, the velocity of rotation, the diameter of the propellers, the velocity and the power of the motor to give the value of C_t for an operational range $5^\circ \leq \varphi \leq 15^\circ$ as is shown in Figure 4. Then, using MatlabTM a first order polynomial (dashed line) can be constructed using the values of the thrust coefficient for each φ angle. The dashed line slope is the derivative of this polynomial which in fact represents the derivative $C_{t_{\varphi}}$, and its value is estimated to be 0.0025.

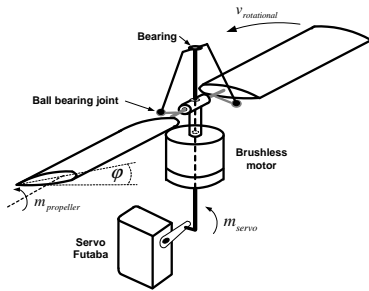


Fig. 3. Schematic of Variable Pitch Propeller (VPP) System

Then using the inertia values given in Table I and applying the Laplace transform, the following transfer function for

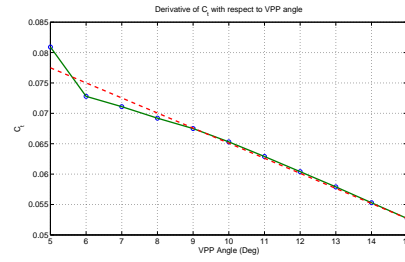


Fig. 4. C_t at different VPP angles

the roll angle with respect to the VPP angle displacement is obtained.

$$\frac{\phi(s)}{\varphi(s)} = \frac{5}{s^2 + 25s} \quad (18)$$

Now, the VPP dynamics will be determined. In the Figure 3, it can be seen that the aerodynamic pitch moment of the blades must be equal to the moment generated by the servo mechanism. Considering that the blade profile corresponds to the NACA0014, then the following approximation can be used to obtain the blade pitch moment:

$$m_b = \frac{\rho V_{t_b}^2 S_b \bar{c}_b}{2 J_{y_b}} [C_{m_{\varphi}} \varphi + C_{m_{\dot{\varphi}}} \dot{\varphi}] = k_s f_s \delta_s \quad (19)$$

where the subscript b denotes the blade. The term V_{t_b} denotes the total velocity of the propeller at the tip, it is given by:

$$V_{t_b} = \sqrt{v_{axial}^2 + v_{rotational}^2} \quad (20)$$

where $v_{rotational} = \pi n D$ and v_{axial} is the aircraft velocity.

The term $C_{m_{\varphi}} = -0.0019$, is the estimated blade pitch moment coefficient slope with respect to φ , being obtained using Javafoil [7], an airfoil analysis shareware software. The term $C_{m_{\dot{\varphi}}} = 1.6 \times 10^{-5}$ is a stability derivative generated by the variation of the VPP rate. The right hand side term of equation (19) represents the moment produced by the servo, where f_s is the force produced by the servo, δ_s is the servo displacement and k_s is a mechanical reduction factor. Using the parameter values in Table I and applying the Laplace transform, yields the VPP dynamic's transfer function:

$$\frac{\varphi(s)}{\delta_s(s)} = \frac{120}{s + 120} \quad (21)$$

The actuator dynamics is given in [8] as follows:

$$\frac{\delta_s(s)}{\delta_c(s)} = \frac{0.6}{0.1s + 1} \quad (22)$$

Then using the transfer functions given previously, the control loop system shown in Figure 5 is proposed to stabilize the roll angle. The system is stable since the characteristic equation $0.1s^4 + 15.5s^3 + 445s^2 + 4260s + 16200$ has all its roots in the left hand side of the complex plane, the roots are located at: $-6.7 \pm 4.5i$, -121 and -20.5 .

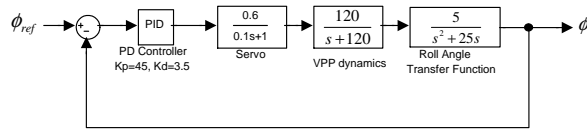


Fig. 5. Roll Control Loop.

B. Pitch control

To obtain the pitch control system the vehicle is considered to be a tailless aircraft flying in forward flight. Assuming that the roll angle is small enough and the roll rate is instantaneously zero, then using (8) and (11), a second order differential equation describing the rotational dynamics for the platform pitch angle can be written as:

$$\ddot{\theta} = m/J_y \quad (23)$$

where m is the pitch moment of the wing, which is given by the following expression:

$$m = \frac{1}{2}V^2\rho S\bar{c}C_m \quad (24)$$

where \bar{c} is the wing chord, S is the wing reference area, V is the airflow speed and C_m is the pitching moment coefficient given by [9]:

$$C_m = C_{m_{ac}} + C_{m_\alpha}\alpha + C_{m_{\delta_e}}\delta_e + C_{m_q}Q\frac{\bar{c}}{V} \quad (25)$$

Assuming that in steady hover flight $\theta = \alpha$ and $C_{m_{ac}} = 0$, then (23) can be reduced to:

$$\ddot{\theta} = \frac{\rho V^2 S \bar{c}}{2J_y} \left[C_{m_\alpha}\theta + C_{m_{\delta_e}}\delta_e + C_{m_q}\frac{\bar{c}}{V}\dot{\theta} \right] \quad (26)$$

The derivative C_{m_α} represents the variation of the pitching moment with respect to the angle-of-attack α . This coefficient depends strongly on the airfoil profile. The derivative $C_{m_{\delta_e}} = \partial C_m / \partial q$ represents the variation of the pitching moment with respect to the elevator control. To estimate these parameters, a shareware software named JavaFoil has been used. This program allows the user to analyze and design, in a rapid and interactive way, a profile over a range of angles of attack [7]. The vehicle main wing has a profile NACA0018 and its pitch moment curves at different angles of attack and elevator positions obtained with this program, are shown in Figure 6. Then $C_{m_\alpha} = -0.145$ and $C_{m_{\delta_e}} = 0.65$. The derivative, $C_{m_q} = -10$, represents the aerodynamic effects due to rotations of the vehicle while the angle of attack remains zero. Using the vehicle parameters given in Table I and the Laplace transform, a second order transfer function representing the pitch angle dynamics is given as follows:

$$\frac{\theta(s)}{\delta_e(s)} = \frac{85}{s^2 + 40s + 18} \quad (27)$$

Then, using the actuator dynamics given previously, a simple proportional derivative compensator with $K_p = 80$ and $K_d = 17$, is proposed to stabilize the pitch angle. This controller stabilizes the platform pitch system because

the roots of the characteristic equation $0.1s^3 + 5s^2 + 908.8s + 4098$ are located at -22.7 ± 91.45 and -4.62 which are in the left hand side of the complex plane.

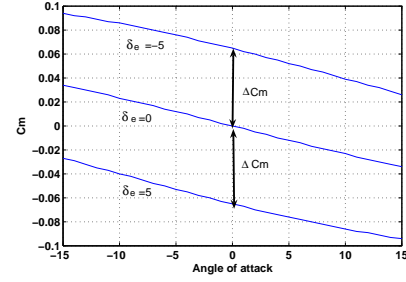


Fig. 6. Pitch moment coefficient curves

C. Yaw control

Now, to control the vehicle yaw position, it is assumed that the pitch and roll angles are stabilized, then the roll rate and pitch rate vanish, then equation (9) can be written as follows:

$$\ddot{\psi} = n/J_z \quad (28)$$

where n is the vehicle yaw moment. Notice that n is used to control yaw during hovering flight and to control roll during forward flight as shown in Figure 7. Under this assumption, the yaw moment can be approximated by the following expression

$$n = \rho V^2 S b C_n / 4 \quad (29)$$

where b is the wing span and C_n is the yawing moment coefficient given by $C_n = C_{n_{\dot{\psi}}} \dot{\psi} + C_{n_{\delta_e}} \delta_e$. Then, (28) can be rewritten as

$$\ddot{\psi} = (\rho V^2 S b) (C_{n_{\dot{\psi}}} \dot{\psi} + C_{n_{\delta_e}} \delta_e) / 4 J_z \quad (30)$$

where $C_{n_{\delta_e}} = 0.19$ represents the variation of the yaw moment with respect to the ailerons positions. $C_{n_{\dot{\psi}}} = 0.19$ is the yaw damping derivative. Applying Laplace transform and using numerical values yields:

$$\frac{\psi(s)}{\delta_e(s)} = \frac{20}{s^2 + 20s} \quad (31)$$

Then, using the actuator dynamics given before, a closed-loop control system with a proportional derivative controller can be proposed, where $K_p = 68$ and $K_d = 17$. The characteristic equation is $0.1s^3 + 3s^2 + 224s + 816$ and its roots are located at $-13 \pm 44.4i$ and -3.8 , therefore the system is stable.

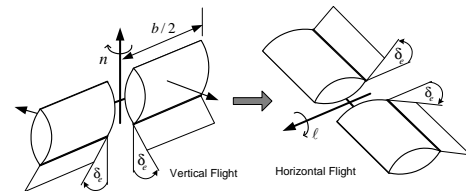


Fig. 7. Yaw Control.

TABLE I
AIRCRAFT PARAMETERS

Parameter	Value	Definition
S	$0.18m^2$	Wing Reference area
\bar{c}	$0.3m$	Wing chord
b	$0.6m$	Wing span
ρ	$1.225kg/m^3$	Air density
V	$10m/s$	Wind velocity (airflow)
J_x	$0.0144kg.m$	x-axis moment of inertia
J_y	$0.0254kg.m$	y-axis moment of inertia
J_z	$0.0312kg.m$	z-axis moment of inertia
d	$0.2m$	Rotor distance from the center of mass
D	0.27	Propeller diameter
n	$9000RPM$	Rotor speed
S_b	$0.006m^2$	Blade reference area
\bar{c}_b	$0.3m$	Blade chord
J_{y_b}	2×10^{-6}	y-axis blade inertia
f_s	$17N$	Force produced by the servo

IV. PLATFORM

The Bidule-CSyRex is a tail-sitter powered by two contra-rotating brushless electric AC motors each driving a variable pitch propeller. Altitude for the vertical flight phases is controlled by collective thrust of the motors. The roll motion in the vertical flight phases is achieved with the difference of thrust between the motors, effect through changing the pitch angle (incidence angle) of the propellers. The vehicle pitch position is controlled by moving the elevons in the same direction while the vertical flight yaw position is controlled by moving the elevons differentially. The elevons are immersed in the propwash of the two propellers for increased effectiveness during the vertical flight phases. The vehicle total weight is about 850 gr, and using two 1250mAh batteries it is possible to have an endurance of approximately 6 minutes in vertical flight. The variable pitch propeller setup has only recently been available commercially and hence would be considered to be an early-generation design with potential performance improvements likely as the concept matures. Theoretical results obtained were incorporated into an autopilot control system using a master-slave architecture based on two 29 MHz Rabbit microcontrollers with 512 Kb Flash and 512Kb RAM, 4 Pulse Wide Modulators (PWM) of 10 bits resolution. These microcontrollers are capable of handle floating point operations and multitasking processing virtually due to the enhancement compiler Dynamic C [10]. The decision to use this architecture was based on the port expansion capability for this prototype, for instance, it is possible to get up to eight PWM ports to control speed of motors, elevons and pitch angle of propellers. A Microstrain inertial measurement unit (IMU) is used to obtain the roll, pitch and yaw angles and angular rates. The inertial information is sent to the master microcontroller which also reads control inputs from the R/C receiver. The master microcontroller subsequently combines this information to calculate the control law and sends the control corrections to the actuators. The servos are used to move the elevons and propeller pitch angles are controlled by the master microcontroller This is done using the PWM port. In the same way, the brushless speed controllers or booster are handled by the slave

microcontroller. The slave microcontroller was configured to add future functionalities such the integration of position sensors, wireless modem, GPS and other mission payload. Figure 8 shows a block diagram of the basic architecture.

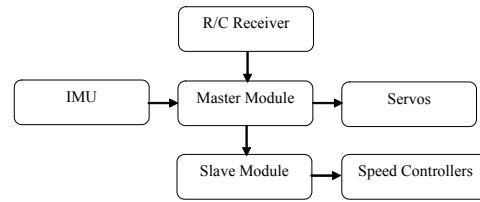


Fig. 8. Architecture

V. RESULTS

A. Simulation

To investigate the behavior of the control stabilization systems, several simulations of the model have been run using Matlab SimulinkTM. This helps to determine the flight handling qualities of the vehicle. For each control loop the step response is evaluated. First, the roll control systems is validated in simulation, this system based in the VPP mechanism has been compared with a roll control system based on the speed variation of the rotors. Normally a control based on the speed variation introduces a time-delay, which is caused by the electronic of the speed controller. This time-delay, provokes instability in the systems making the tuning of the controller parameters a very difficult task. Figure 9 shows the comparison of the two systems. The two systems reach the desired value almost at the same time, but in the system using speed variation there are oscillations in the steady state, while the VPP control quickly stabilizes the system. In the same way, the step response for the pitch and yaw closed-loop control systems have been simulated. Their respective responses are shown in Figures 10 and 11.

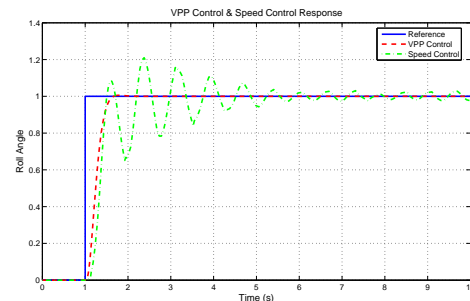


Fig. 9. Response of the Roll Control Loop

B. Experimental

In this section, qualitative results in flight test of the tail-sitter are discussed. This vehicle in vertical flight presents a natural unstable behavior, and the manual guidance and control is a very difficult task even if the remote human operator has an excellent piloting skill. Figure 12 shows the vehicle crashing due to the high instability in a test without any automatic control algorithm.

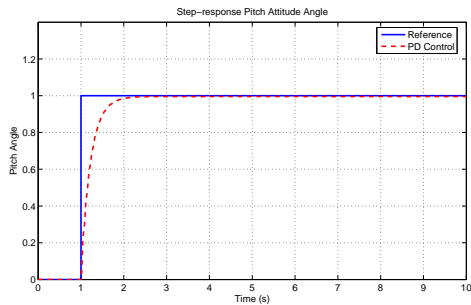


Fig. 10. Response of the Pitch Control Loop

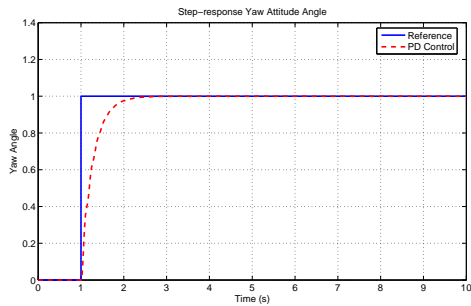


Fig. 11. Response of the Yaw Control Loop

As it was seen in previous sections, the control law for this vehicle is a simple PD control, which has been chosen due that the position variables and its derivatives are obtained directly from the IMU. The integral is avoided due to the high probability for error in the steady state because of the signal noise in the sensors. To adjust the control parameters several flight tests were carried out until obtaining a good performance of the vehicle. First the K_d gains were adjusted to get a good stiffness in all the angular displacements, then the K_p gain was adjusted to obtain a good time response to changes of angular position. The stability derivatives, C_{l_ϕ} , C_{m_q} , $C_{n_{\delta_e}}$, $C_{n_{\dot{\psi}}}$ and $C_{m_{\dot{\phi}}}$ would normally be estimated using the data obtained from wind tunnel tests. However, in the current study first the controller parameters were first obtained in flight test, then using the values of the derivatives and the aerodynamic coefficients estimated using Javafoil and Javaprop, the unknown derivatives were obtained. Figure 13 shows the vehicle flying stable when the linear control PD is used. Note that tethers were used for safety purposes only, with satisfactory flight test results used only when all



Fig. 12. Bidule-CSyRex with no control

the tether are slack, thus not supporting the flight platform in any way.

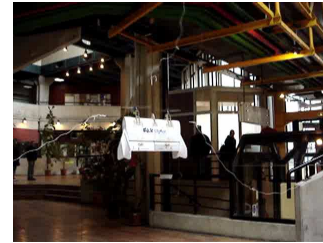


Fig. 13. Bidule-CSyRex with PD control

VI. CONCLUSIONS AND FUTURE WORKS

A simplified aerodynamic model for a tail-sitter mAV has been developed using the Newton-Euler formulation. A variable pitch propeller control has been used for roll control of a tail-sitter in vertical flight phases with good results. Experimental tests confirmed that the tail-sitter aerodynamic configuration is very complex and unstable. This means that even experienced pilots can not manually stabilize this type of aircraft during hovering. Linear PD controllers have been proposed for stabilizing the pitch, roll and yaw of the flight platform. This controller has been successfully proved experimentally. Future work in this area includes obtaining a higher fidelity aerodynamical model and exploring different nonlinear control algorithms. In addition, transition to horizontal flight will be investigated with implementation of guidance controllers to investigate mission capabilities of the platform. The presented work highlights the high potential for a versatile mAV flight platform in flight control research.

VII. ACKNOWLEDGMENTS

Authors are thankful to the Universidad Autonoma de Tamps., México, CNRS-UTC, France and The University of Sydney, Australia.

REFERENCES

- [1] P. Castillo, *Modelling and Control of Miniflying Machines*, Springer, London; 2005.
- [2] H. Stone, "Aerodynamic Modelling of a Wing-in-Slipstream Tail-sitter UAV", in *AIAA Biennial International Powered Lift Conference and Exhibit*, Williamsburg, Virginia, 2002.
- [3] W. Green and P. Oh, "Autonomous Hovering of a Fixed-Wing Micro Air Vehicle", in *Proceedings of the 2006 IEEE International Conference on Robotics and Automation*, Orlando, Florida, 2006, pp 2164-2169.
- [4] P.V. Blyenburg, *UAVs Systems, The Global Perspective*, UVS International, 2006, www.uvs-info.com.
- [5] Sperry and K.C. Wong, "Design and development of a micro air vehicle (mAV) concept: Project Bidule", in *9th Australian International Aerospace Congress (AIAC)*, Canberra, Australia, 2001.
- [6] B.L. Stevens and F.L. Lewis, *Aircraft Control and Simulation*, John Wiley and Sons, New Jersey USA; 2003.
- [7] M. Hepperle, *Aerodynamics for Model Aircraft*, 2006, <http://www.mh-aerotoools.de>.
- [8] N. Kannan et M.Seetharama Bhat, "Longitudinal H_∞ Stability Augmentation System for a Thrust-Vectored Unmanned Aircraft", in *AIAA Journal of Guidance, Control and Dynamics*, Vol. 28, No.6, page 1240.
- [9] Bernard Etkin and Lloyd Duff Reid, *Dynamics of Flight Stability and Control*, John Wiley and Sons; 1996.
- [10] Rabbit Semiconductors, *Dynamics C user manual*, 2007, <http://www.rabbitsemiconductor.com/>.